

# Experimental constraints on the neutrino and gauge parameters of the super-weak U(1) extension of the standard model

Timo J. Kärkkäinen\*

*Institute for Theoretical Physics, ELTE Eötvös Loránd University,  
Pázmány Péter sétány 1/A, 1117 Budapest, Hungary*

Zoltán Trócsányi†

*Institute for Theoretical Physics, ELTE Eötvös Loránd University,  
Pázmány Péter sétány 1/A, 1117 Budapest, Hungary and  
ELKH-DE Particle Physics Research Group, University of Debrecen  
4010 Debrecen, PO Box 105, Hungary*

(Dated: 26.05.2021)

## Abstract

The super-weak force is a minimal, anomaly-free U(1) extension of the standard model (SM), designed to explain the origin of (i) neutrino masses and mixing matrix elements, (ii) dark matter, (iii) cosmic inflation, (iv) stabilization of the electroweak vacuum and (v) leptogenesis. We discuss the neutrino sector of this model in detail and study the allowed parameter space of the neutrino Yukawa matrices and mixing matrix elements. The model generates nonstandard neutrino interactions, whose allowed experimental limits are used to constrain the parameter space of the model. We provide benchmark points in the relevant parameter space that fall within the sensitivity region of the SHiP and MATHUSLA experiments.

---

\* timo.karkkainen@ttk.elte.hu

† Zoltan.Trocsanyi@cern.ch

# Contents

I. Introduction	3
II. Model description	4
A. Gauge extension	4
B. New neutral currents	6
C. Scalar extension	7
D. Neutrino extension	8
III. Neutrino masses and mixing	9
A. Seesaw expansion	10
B. Diagonalization of the light neutrino mass matrix at one loop	11
C. Parametrization of the mass matrix	13
IV. Nonstandard interactions	16
A. Nonstandard interactions in medium	18
B. Changes to the neutrino-electron elastic scattering	20
V. Benchmark points	22
VI. Conclusions	25
A. Flavour-universal NSI and non-unitary mixing	29
B. Light NSI mediator	30
References	30

# I. Introduction

Finding all the building blocks of the standard model (SM) of elementary particle interactions has been an effort spanning nearly half a century, concluding with the discovery of the Higgs boson in 2012 [1, 2]. During that time several hints and discoveries have unfolded, confirming that the SM cannot describe all observations in particle physics. In this post-SM era, several simple extensions of the SM are experiencing a renaissance as the number of reported deviations from the SM in particle physics are increasing [3, 4]. The discovery of the in-flight flavour oscillation of neutrinos [5, 6] in vacuum and matter requires that at least two of the three known neutrinos must have non-vanishing masses. However, the SM is devoid of a suitable mass generation mechanism for the neutrinos. To counter this, the existence of right-handed neutrinos that are sterile under the standard model gauge group have been proposed. The seesaw mechanism [7–11] utilizes these neutrinos that mix weakly with the active ones. Sterile neutrinos have been considered as dark matter candidates [12–21], and their role for the baryonic asymmetry of the universe via leptogenesis has been studied intensively, see for instance [12, 14, 22]. An unidentified 3.5 keV X-ray line discovered in Andromeda galaxy and several galaxy clusters [23, 24] may be interpreted to originate from sterile neutrino decays at one-loop order in perturbation theory, with the mass of sterile neutrino being about 7.1 keV<sup>1</sup> and mixing very weakly with the active ones, with mixing angle  $O(10^{-11})$ .

Light sterile neutrinos at keV range have been searched by several experiments [25] measuring the electron energy spectrum of unstable  $\beta$  decaying nuclei. The sterile component of  $\nu_e$  would cause missing events and a kink concentrated at  $E_{\text{max}}^e - m_s$ , where  $m_s$  is the mass of sterile neutrino and  $E_{\text{max}}^e$  is the endpoint of electron energy spectrum. These *kink searches* have ruled out a mixing larger than  $|U_{e4}|^2 = O(10^{-3})$ . MeV scale neutrinos are sensitive to peak searches, where a meson decay is enhanced by the sterile neutrino. Mixing larger than  $|U_{e4}|^2 = O(10^{-5})$  has been ruled out on 10–100 MeV mass range [26–29]. Even heavier neutrinos of mass  $O(1)$  GeV are constrained by beam dump experiments, with CHARM constraining  $|U_{e4}|^2 \lesssim 10^{-6}$  for sterile neutrinos in the 0.5–2 GeV mass range [30]. Searches for sterile neutrinos of larger masses in decays of the  $Z^0$  boson have been performed

---

<sup>1</sup> We use natural units in this paper.

by DELPHI [31], constraining  $|U_{e4}|^2 \lesssim 10^{-5}$  for sterile neutrino mass range 2–60 GeV.

New physics in the neutrino sector can be parameterized via the nonstandard interaction (NSI) formalism [32], which produces distortions to neutrino oscillation spectra and neutrino scattering experiments. The NSI operators can be generated at the effective theory level in theories which couple new fields to active neutrinos. Particularly a new U(1) gauge boson may couple to neutrinos if they have suitable U(1) charge assignments. In this paper we explore such a possibility within the model of the super-weak force [33]. We study how the experimental limits on the NSI constrain the parameter space. We also demonstrate that the model provides benchmark points in the allowed parameter region that fall in the sensitivity region of future experiments searching for sterile neutrinos.

The structure of this paper is as follows. In Sec. II, we present a description of the super-weak model. Neutrino mass generation, mixing and sub-leading corrections to neutrino mass are covered in Sec. III. Nonstandard neutrino interactions are derived and constrained in Sec. IV. We present our benchmark points and results in Sec. V, and give our conclusions in Sec. VI.

## II. Model description

In the super-weak extension of the SM [33], the field content is enlarged by one complex singlet scalar and three right-handed fermion fields that become massive sterile neutrinos after spontaneous symmetry breaking. Here we recall the details of the gauge, scalar and fermion sectors to the extent we need for our analysis.

### A. Gauge extension

The underlying gauge group of the model is

$$G = \text{SU}(3)_c \otimes \text{SU}(2)_L \otimes \text{U}(1)_Y \otimes \text{U}(1)_z, \quad (\text{II.1})$$

which is anomaly-free with the quantum numbers given in Table I. The covariant derivative for the matter field  $f$  is defined as

$$D_f^\mu = \partial^\mu + ig_L \mathbf{T} \cdot \mathbf{W}^\mu + iy_f g_y B^\mu + iz_f g_z Z^\mu, \quad (\text{II.2})$$

where  $g_L$ ,  $g_y$  and  $g_z$  are the gauge couplings of corresponding gauge groups. (We omit the  $SU(3)_c$  part in our description, since it is not relevant in our discussion.) The corresponding gauge fields are  $\mathbf{W}^\mu = (W_1^\mu, W_2^\mu, W_3^\mu)$ ,  $B^\mu$  and  $Z^\mu$ . The charges  $y_f$  and  $z_f$  correspond to  $U(1)_Y$  and  $U(1)_z$  groups, and  $\mathbf{T} = (T^1, T^2, T^3)$  are the generators of the  $SU(2)_L$  group (1/2 times the Pauli matrices).

Table I. Gauge group representations and charges of the fermions and scalars in the super-weak model

Field	$SU(3)_c$	$SU(2)_L$	$U(1)_Y$	$U(1)_z$
$Q_L$	<b>3</b>	<b>2</b>	$\frac{1}{6}$	$\frac{1}{6}$
$u_R$	<b>3</b>	<b>1</b>	$\frac{2}{3}$	$\frac{7}{6}$
$d_R$	<b>3</b>	<b>1</b>	$-\frac{1}{3}$	$-\frac{5}{6}$
$L_L$	<b>1</b>	<b>2</b>	$-\frac{1}{2}$	$-\frac{1}{2}$
$\ell_R$	<b>1</b>	<b>1</b>	$-1$	$-\frac{3}{2}$
$N_R$	<b>1</b>	<b>1</b>	$0$	$\frac{1}{2}$
$\phi$	<b>1</b>	<b>2</b>	$\frac{1}{2}$	$1$
$\chi$	<b>1</b>	<b>2</b>	$0$	$-1$

The gauge kinetic terms of the Lagrangian,

$$\mathcal{L}_{\text{gauge}} = -\frac{1}{4}B^{\mu\nu}B_{\mu\nu} - \frac{1}{4}Z^{\mu\nu}Z_{\mu\nu} - \frac{1}{4}\mathbf{W}^{\mu\nu} \cdot \mathbf{W}_{\mu\nu} - \frac{\varepsilon}{2}B_{\mu\nu}Z^{\mu\nu} \quad (\text{II.3})$$

include a kinetic mixing term, proportional to a real parameter  $\varepsilon \ll 1$ . We can redefine the  $U(1)$  fields via a linear transformation

$$\begin{pmatrix} \hat{B}_\mu \\ \hat{Z}_\mu \end{pmatrix} = \begin{pmatrix} 1 & \sin \theta_\varepsilon \\ 0 & \cos \theta_\varepsilon \end{pmatrix} \begin{pmatrix} B_\mu \\ Z_\mu \end{pmatrix}, \quad \sin \theta_\varepsilon \equiv \varepsilon. \quad (\text{II.4})$$

Then the covariant derivative can be rewritten as

$$D_f^\mu = \partial^\mu + ig_L \mathbf{T} \cdot \mathbf{W}^\mu + i(y, z)_f \begin{pmatrix} g_y & -g'_y \\ 0 & g'_z \end{pmatrix} \begin{pmatrix} \hat{B}_\mu \\ \hat{Z}_\mu \end{pmatrix}, \quad (\text{II.5})$$

where  $g'_y = g_y \tan \theta_Z$  and  $g'_z = g_z / \cos \theta_Z$ . In this basis the kinetic mixing is absent, which can be achieved but at an arbitrarily chosen scale. The scale dependence of the mixing term is mild [21], hence we neglect it in this exploratory paper and will study its effect in a more

complete analysis. The  $\hat{Z}$  and  $\hat{B}$  fields being both electrically neutral can still mix with the neutral  $W_3$  boson via a rotation:

$$\begin{pmatrix} W_\mu^3 \\ \hat{B}_\mu \\ \hat{Z}_\mu \end{pmatrix} = \begin{pmatrix} \cos \theta_W \cos \theta_Z & \cos \theta_W \sin \theta_Z & \sin \theta_W \\ -\sin \theta_W \cos \theta_Z & -\sin \theta_W \sin \theta_Z & \cos \theta_W \\ -\sin \theta_Z & \cos \theta_Z & 0 \end{pmatrix} \begin{pmatrix} Z_\mu \\ Z'_\mu \\ A_\mu \end{pmatrix}, \quad (\text{II.6})$$

where the Weinberg angle  $\theta_W$  is defined as in the SM. The second mixing angle  $\theta_Z$  mixes the massive fields and is determined by the relation

$$\tan 2\theta_Z = -\frac{2(2g'_z - g'_y)\sqrt{g_L^2 + g_y^2}}{g_L^2 + g_y^2 - (2g'_z - g'_y)^2 - 4g_z'^2 \tan^2 \beta} \quad (\text{II.7})$$

where  $\tan \beta = w/v$  is the ratio of the vacuum expectation values (VEVs) of the scalar fields (see Eq. (II.20)). The extra degree of freedom introduced by the  $U(1)_z$  group manifests itself as an extra neutral massive gauge boson, which we call the  $Z'$  boson. It mixes with the  $Z$  boson, the other massive neutral gauge boson in the model.

## B. New neutral currents

All fermions have  $z$ -charges, which lead to new neutral currents  $\bar{f} \Gamma_{Z'ff}^\mu f$  coupled to the  $Z'_\mu$ . The coupling of the  $Z'$  boson to fermion fields  $f = \nu, \ell, u, d$  has the form [33]

$$\Gamma_{Z'ff}^\mu = -ie\gamma^\mu (C_{Z'ff}^R P_R + C_{Z'ff}^L P_L) \quad (\text{II.8})$$

where  $P_{L,R} = \frac{1}{2}(1 \mp \gamma_5)$  are chiral projection operators and

$$C_{Z'ff}^R = -g_f^+ \sin \theta_Z + h_f^+ \cos \theta_Z, \quad C_{Z'ff}^L = -g_f^- \sin \theta_Z + h_f^- \cos \theta_Z. \quad (\text{II.9})$$

The coupling factors are

$$g_f^+ = -\frac{\sin \theta_W}{\cos \theta_W} e_f, \quad g_f^- = \frac{T_f^3 - \sin^2 \theta_W e_f}{\sin \theta_W \cos \theta_W}, \quad h_f^\pm = \frac{g'_Z R_f^\pm + (g'_z - g'_y)(e_f - R_f^\mp)}{g_L \sin \theta_W}, \quad (\text{II.10})$$

Table II. Table of all the couplings for different fields.

field	$e_f$	$T_f^3$	$R_f^+$	$R_f^-$
$u, c, t$	$\frac{2}{3}$	$\frac{1}{2}$	$\frac{1}{2}$	0
$d, s, b$	$-\frac{1}{3}$	$-\frac{1}{2}$	$-\frac{1}{2}$	0
$\nu_e, \nu_\mu, \nu_\tau$	0	$\frac{1}{2}$	$\frac{1}{2}$	0
$e^-, \mu^-, \tau^-$	-1	$-\frac{1}{2}$	$-\frac{1}{2}$	0

with values of  $e_f, T_f^3, R_f^+$  and  $R_f^-$  given in Table II. Explicit computations yield

$$eC_{Z'\nu\nu}^L = \frac{1}{2}(g'_y - g'_z) \cos \theta_Z - \frac{g_L}{2} \frac{\sin \theta_Z}{\cos \theta_W}, \quad eC_{Z'\nu\nu}^R = \frac{g'_z}{2} \cos \theta_Z, \quad (\text{II.11})$$

$$eC_{Z'\ell\ell}^L = \frac{1}{2}(g'_y - g'_z) \cos \theta_Z + \frac{g_L}{2} \frac{1 - 2 \sin^2 \theta_W}{\cos \theta_W} \sin \theta_Z, \quad (\text{II.12})$$

$$eC_{Z'\ell\ell}^R = \left(g'_y - \frac{3}{2}g'_z\right) \cos \theta_Z - g_L \frac{\sin^2 \theta_W}{\cos \theta_W} \sin \theta_Z, \quad (\text{II.13})$$

$$eC_{Z'uu}^L = -\frac{1}{6}(g'_y - g'_z) \cos \theta_Z - \frac{1}{6}g_L \frac{3 - 4 \sin^2 \theta_W}{\cos \theta_W} \sin \theta_Z, \quad (\text{II.14})$$

$$eC_{Z'uu}^R = -\frac{1}{6}(4g'_y - 7g'_z) \cos \theta_Z + \frac{2}{3}g_L \frac{\sin^2 \theta_W}{\cos \theta_W} \sin \theta_Z, \quad (\text{II.15})$$

$$eC_{Z'dd}^L = -\frac{1}{6}(g'_y - g'_z) \cos \theta_Z + \frac{1}{6}g_L \frac{3 - 2 \sin^2 \theta_W}{\cos \theta_W} \sin \theta_Z, \quad (\text{II.16})$$

$$eC_{Z'dd}^R = \frac{1}{6}(2g'_y - 5g'_z) \cos \theta_Z - \frac{1}{3}g_L \frac{\sin^2 \theta_W}{\cos \theta_W} \sin \theta_Z \quad (\text{II.17})$$

The couplings  $C_{Z'ff}^{L/R}$  are real because the gauge couplings are themselves real.

### C. Scalar extension

The scalar sector of the model consists of a complex doublet  $\phi = \begin{pmatrix} \phi^+ \\ \phi^0 \end{pmatrix}$  and a complex singlet  $\chi$ . The scalar Lagrangian can be written as

$$\mathcal{L}_{\text{scalar}} = (D_\mu \phi)^* (D^\mu \phi) + |D_\mu \chi|^2 - \mu_\phi^2 \phi^\dagger \phi - \mu_\chi^2 |\chi|^2 - \lambda_\phi (\phi^\dagger \phi)^2 - \lambda_\chi |\chi|^4 - \lambda (\phi^\dagger \phi) |\chi|^2, \quad (\text{II.18})$$

up to a constant term irrelevant to our discussion. All the couplings are real. The portal coupling  $\lambda$  induces mixing between the neutral component of  $\phi$  and  $\chi$ . The potential is minimal at the scalar field values

$$\phi_0 = \frac{1}{\sqrt{2}} \begin{pmatrix} 0 \\ v \end{pmatrix}, \quad \chi_0 = \frac{w}{\sqrt{2}}, \quad (\text{II.19})$$

where

$$\frac{v}{\sqrt{2}} = \sqrt{\frac{2\lambda_\chi\mu_\phi^2 - \lambda\mu_\chi^2}{4\lambda_\phi\lambda_\chi - \lambda^2}}, \quad \frac{w}{\sqrt{2}} = \sqrt{\frac{2\lambda_\phi\mu_\chi^2 - \lambda\mu_\phi^2}{4\lambda_\phi\lambda_\chi - \lambda^2}}. \quad (\text{II.20})$$

In this paper we perform our analyses at tree level, hence we can choose the unitary gauge, in which after spontaneous symmetry breaking (SSB) the fields  $\phi$  and  $\chi$  can be parametrized in terms of two real scalar fields  $h'$  and  $s'$  as

$$\phi = \frac{1}{\sqrt{2}} \begin{pmatrix} 0 \\ v + h' \end{pmatrix} \quad \text{and} \quad \chi = \frac{1}{\sqrt{2}}(w + s'). \quad (\text{II.21})$$

The mass matrix for scalars in  $(h', s')$  basis is given by

$$M_{ij}^{\text{scalar}} = \begin{pmatrix} 3\lambda_\phi v^2 + \frac{1}{2}\lambda w^2 + \mu_\phi^2 & \lambda v w \\ \lambda v w & 3\lambda_\chi w^2 + \frac{1}{2}\lambda v^2 + \mu_\chi^2 \end{pmatrix}, \quad (\text{II.22})$$

which has eigenvalues

$$M_{h_\pm}^2 = \lambda_\phi v^2 + \lambda_\chi w^2 \pm \sqrt{(\lambda_\phi v^2 - \lambda_\chi w^2)^2 + (\lambda v w)^2}. \quad (\text{II.23})$$

We adopt the convention  $M_{h_-} \leq M_{h_+}$ . Diagonalizing the mass matrix with an orthogonal rotation  $O_S$ , we obtain the mass eigenstates  $h$  and  $s$ :

$$\begin{pmatrix} h \\ s \end{pmatrix} = \begin{pmatrix} \cos \theta_S & -\sin \theta_S \\ \sin \theta_S & \cos \theta_S \end{pmatrix} \begin{pmatrix} h' \\ s' \end{pmatrix} \quad (\text{II.24})$$

where the scalar mixing angle is given by

$$\tan 2\theta_S = -\frac{\lambda v w}{\lambda_\phi v^2 - \lambda_\chi w^2} \equiv -\frac{\lambda \tan \beta}{\lambda_\phi - \lambda_\chi \tan^2 \beta}, \quad (\text{II.25})$$

with  $\tan \beta = w/v$ . The correspondence between the states  $(h_+, h_-)$  and  $(h, s)$  depends on the sign of  $\theta_S$ , which can be determined experimentally by the hierarchy between the masses of the Higgs particle and the new scalar particle. It was shown in Ref. [34] that the stability of the vacuum is assured up to the Planck scale within the super-weak model if the SM Higgs particle is lighter than the new scalar.

#### D. Neutrino extension

The fermion sector of the SM is extended by three massive right-handed neutrinos that are charged under  $U(1)_z$  only, i.e. sterile under the SM gauge group. They can have either



Dirac or Majorana nature. Since the Yukawa term that produces the Majorana mass term for Dirac-type neutrinos is allowed by the gauge symmetries, we include both Dirac- and Majorana-type Yukawa terms in the Lagrangian.

We write the leptonic part of the Yukawa Lagrangian as

$$-\mathcal{L}_Y^\ell = \frac{1}{2} \overline{(N_R)^c} Y_N \chi^* N_R + \overline{L_L} \phi Y_\ell \ell_R + \overline{L_L} \phi^c Y_\nu N_R + \text{h.c.} \quad (\text{II.26})$$

where the fermion fields are triplets in flavour space,

$$N_R = \begin{pmatrix} N_1 \\ N_2 \\ N_3 \end{pmatrix}, \quad L_L = \begin{pmatrix} L_{Le} \\ L_{L\mu} \\ L_{L\tau} \end{pmatrix}, \quad \ell_R = \begin{pmatrix} e_R \\ \mu_R \\ \tau_R \end{pmatrix}. \quad (\text{II.27})$$

The superscript  $c$  denotes charge conjugation,  $\varphi^c = i\sigma_2 \varphi^*$  for a generic two-component field  $\varphi$  (left-handed Weyl spinor or complex scalar doublet).

We can *choose* to work on a basis where the  $Y_N$  and  $Y_\ell$  are diagonal matrices, corresponding to mass eigenstates of the lepton fields  $N$  and  $\ell$ . Before diagonalization, i.e. on the flavour basis, the Majorana-type Yukawa matrix  $Y'_N$  was symmetric, so the diagonalizing matrix  $O_N$  is orthogonal. In contrast, the charged lepton Yukawa matrix  $Y'_\ell$  is diagonalized via biunitary transformation, using two unitary matrices  $U_{\ell L}$  and  $U_{\ell R}$ :

$$Y_N = O_N^T Y'_N O_N, \quad Y'_\ell = U_{\ell L}^\dagger Y'_\ell U_{\ell R}. \quad (\text{II.28})$$

In this context, we define the corresponding Dirac neutrino Yukawa matrix to be  $Y_\nu \equiv Y'_\nu O_N$  without losing generality.

After SSB, the Yukawa Lagrangian of the leptons becomes

$$-\mathcal{L}_Y^\ell = \frac{w + s'}{2\sqrt{2}} \overline{(N_R)^c} Y_N N_R + \frac{v + h'}{\sqrt{2}} \overline{\ell_L} Y_\ell \ell_R + \frac{v + h'}{\sqrt{2}} \overline{\nu_L} Y_\nu N_R + \text{h.c.} \quad (\text{II.29})$$

### III. Neutrino masses and mixing

In this section we review a possible parametrization of the type-I seesaw mechanism within the super-weak model. While it is very similar to the standard in the literature, we present it explicitly in the form that we shall use later to find benchmark points.

### A. Seesaw expansion

First we identify the neutrino mass matrix from Eq. (II.29), and write it in the full  $6 \times 6$  form:

$$-\mathcal{L}_m^\nu = \frac{1}{2} \begin{pmatrix} \nu_L \\ (N_R)^c \end{pmatrix}^T \begin{pmatrix} 0 & m_D \\ m_D^T & m_R \end{pmatrix} \begin{pmatrix} (\nu_L)^c \\ N_R \end{pmatrix} + \text{h.c.}, \quad (\text{III.1})$$

where  $\nu_L$  is a similar triplet as  $N_R$  defined in Eq. (II.27), while the Dirac and Majorana neutrino mass terms are

$$m_D = \frac{v}{\sqrt{2}} Y_\nu \quad \text{and} \quad m_R = \frac{w}{\sqrt{2}} Y_N. \quad (\text{III.2})$$

Then we can block-diagonalize the block mass matrix up to small corrections:

$$\begin{pmatrix} m_\nu & 0 \\ 0 & m_N \end{pmatrix} = \begin{pmatrix} I & U_{as} \\ -U_{as}^\dagger & I \end{pmatrix}^T \begin{pmatrix} 0 & m_D \\ m_D^T & m_R \end{pmatrix} \begin{pmatrix} I & U_{as} \\ -U_{as}^\dagger & I \end{pmatrix} \approx \begin{pmatrix} -m_D m_R^{-1} m_D^T & 0 \\ 0 & m_R \end{pmatrix} \quad (\text{III.3})$$

where

$$U_{as} = m_D^* m_R^{-1\dagger} = \begin{pmatrix} U_{e4} & U_{e5} & U_{e6} \\ U_{\mu 4} & U_{\mu 5} & U_{\mu 6} \\ U_{\tau 4} & U_{\tau 5} & U_{\tau 6} \end{pmatrix}, \quad (\text{III.4})$$

so

$$m_D = U_{as}^* m_R, \quad m_D^T = m_R U_{as}^\dagger. \quad (\text{III.5})$$

In the last step of (III.3) we neglected blocks suppressed by powers of  $m_D$ , such as the off-diagonal blocks  $U_{as}^* m_D^T U_{as}$  and its transpose. Those matrices have small elements for all benchmark points in our discussion during the next sections essentially because there are stringent bounds on the elements of the active-sterile mixing matrix in the mass range 1–80 GeV of the sterile neutrinos:  $|U_{ai}|^2 \lesssim 10^{-5}$  ( $a = e, \mu, \tau, i = 4, 5, 6$ ) [35, 36].

We also neglected terms in the seesaw expansion from the diagonal block  $m_N$ . The order of magnitude of such a correction to a sterile neutrino of mass in the keV range is

$$\Delta m_N \sim (m_D^T m_D^* m_R^{-1})_{ii} = \frac{v^2 (Y_\nu^T Y_\nu^*)_{ii}}{2 (m_R)_{ii}} \simeq \frac{(Y_\nu^T Y_\nu^*)_{ii}}{10^{-19}} \times \frac{\text{keV}}{(m_N)_{ii}} \times 6 \text{ eV}, \quad (\text{III.6})$$

which is much smaller than the keV scale for all our benchmarks with one exception where numerical coincidence leads to moderately large correction of 1.3 keV. (The actual size of the correction terms can be calculated using our benchmark Yukawa matrices  $Y_\nu$ , with values

given in Sect. V.) The corrections to a GeV sterile neutrino mass are larger by one order of magnitude. Thus we can safely drop the neglected terms.

A similar term emerges also for the light neutrino mass matrix as sub-leading order terms from seesaw expansion. Within second order, these are [37]

$$\Delta m_\nu = \frac{1}{2} m_\nu m_D^\dagger m_N^{-2} m_D + \frac{1}{2} \left( m_\nu m_D^\dagger m_N^{-2} m_D \right)^T \quad (\text{III.7})$$

By direct calculation for the benchmark points, this correction turns out to be much smaller than  $10^{-7}$  eV (see Table III), so our approximations in the seesaw expansion are justified. As a result  $m_\nu \approx -m_D m_R^{-1} m_D^T$  and  $m_N \approx m_R$  are the approximate mass matrices for active and sterile neutrinos.

## B. Diagonalization of the light neutrino mass matrix at one loop

At this point  $m_N$  is already diagonal, but  $m_\nu$  is not so, so next we diagonalize the light neutrino mass matrix  $m_\nu$ :

$$\begin{pmatrix} U_2 & 0 \\ 0 & I \end{pmatrix}^T \begin{pmatrix} m_\nu & 0 \\ 0 & m_N \end{pmatrix} \begin{pmatrix} U_2 & 0 \\ 0 & I \end{pmatrix} = \begin{pmatrix} U_2^T m_\nu U_2 & 0 \\ 0 & m_N \end{pmatrix} = \begin{pmatrix} m_\nu^{\text{diag}} & 0 \\ 0 & m_N^{\text{diag}} \end{pmatrix}, \quad (\text{III.8})$$

where  $U_2$  is a  $3 \times 3$  unitary matrix. We have experimental constraints on the upper limits the elements of  $m_\nu^{\text{diag}}$  [38, 39]. Even if the tree-level matrix  $m_\nu^{\text{diag}}$  satisfies those limits, one has to check that the inclusion of loop corrections do not upset them.

Due to the active-sterile mixing of neutrinos, the one-loop correction to light neutrino masses has contributions involving right-handed neutrinos and neutral scalars or vector bosons in the loop. The required computations in the context of gauged U(1) extensions of the standard model is documented in Ref. [40]. Here we simply recall the total one-loop correction for the super-weak model:

$$\begin{aligned} (\delta m_\nu)_{ij} = & \sum_{V=Z,Z'} \frac{3e^2}{16\pi^2 M_V^2} \left( C_{V\nu\nu}^L - C_{V\nu\nu}^R \right)^2 \sum_{n=1}^6 (U_L^*)_{in} m_n^3 \frac{\ln \frac{m_n^2}{M_V^2}}{\frac{m_n^2}{M_V^2} - 1} (U_L^\dagger)_{nj} \\ & + \frac{1}{16\pi^2 v^2} \sum_{n=1}^6 (U_L^*)_{in} m_n^3 (U_L^\dagger)_{nj} \left( \sin^2 \theta_S \frac{\ln \frac{m_n^2}{M_s^2}}{\frac{m_n^2}{M_s^2} - 1} + \cos^2 \theta_S \frac{\ln \frac{m_n^2}{M_h^2}}{\frac{m_n^2}{M_h^2} - 1} \right) \end{aligned} \quad (\text{III.9})$$

where the summation runs over all six neutrinos<sup>2</sup> and the  $U_L = (U_2 \ U_{\text{as}})$  matrix is the upper  $(3 \times 6)$  part of the unitary matrix that diagonalizes the full neutrino mass matrix.

<sup>2</sup> Here  $\nu_i = N_{i-3}$  for  $i > 3$ .

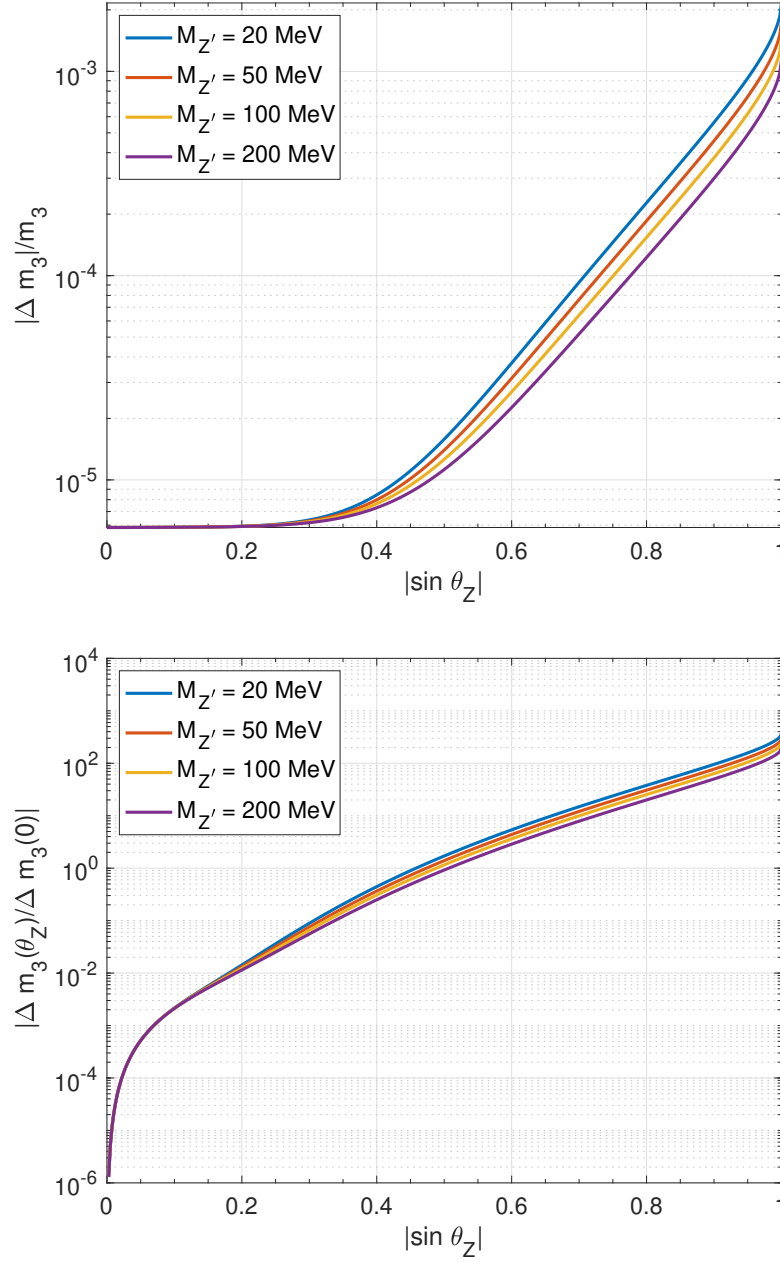


Figure 1. One-loop corrections to the mass of  $\nu_3$ , corresponding to **BP1** (see Sect. V for precise definition), with  $\text{sgn}(\theta_Z) = +1$ ,  $M_s = 250 \text{ GeV}$  and  $\sin \theta_S = 0.1$ . Top: relative correction to  $\nu_3$  mass. Bottom: correction relative to case  $\theta_Z = 0$ .

The correction to the mass of  $\nu_3$  (the heaviest of the light neutrinos, assuming normal mass hierarchy  $m_1 < m_2 < m_3$ , and obtained by diagonalization of the corrected mass matrix  $m_\nu + \delta m_\nu$ ) due to only the  $Z'$  boson is shown in Fig. 1, denoted by  $\Delta m_3$ . Looking

at the figure, it is clear that the one-loop correction is tiny compared to the mass of  $\nu_3$  with our choice of  $|\sin \theta_Z| \ll 1$ , relevant to the super-weak case. We consider the mass range  $M_{Z'} \in [20, 200]$  MeV where the lightest right-handed neutrino may be sufficiently abundant to provide the correct dark matter energy density with freeze-out scenario [21]. The smaller  $M_{Z'}$  the larger correction.

In the lower plot of Fig. 1 we show the full correction as a function of  $\theta_Z$ ,  $\Delta m_3(\theta_Z)$ , relative to the case  $\theta_Z = 0$ , which corresponds to the  $Z'$  boson playing no role in neutrino interactions. It demonstrates how the correction  $\Delta m_3$  is dominated by the  $Z'$  loop only when  $|\sin \theta_Z| \gtrsim 0.5$ . Fig. 2 shows that the shapes of the plots are similar for  $\nu_1$  and  $\nu_2$ , so we can make the same conclusions for those neutrinos.

The effect of loop corrections on the neutrino oscillation parameters is similarly small, and the relative correction for the squared mass differences is approximately the mass correction squared, as can be seen from Fig. 3. Fig. 4 shows the contours of relative one-loop corrections to the mass of  $\nu_3$  as a function of the masses of the  $N_2$  neutrino (recall that  $m_5 \approx m_6$ ) and  $Z'$ . We see that for  $m_5 < 100$  GeV and  $M_{Z'} < 10^5$  GeV the loop corrections are very small.

### C. Parametrization of the mass matrix

Having established the validity of the mass matrix (III.8), we use the Casas-Ibarra parameterization [41] to write the diagonalized light neutrino mass matrix as

$$m_\nu^{\text{diag}} = U_2^T m_\nu U_2 = -U_2^T m_D m_R^{-1} m_D^T U_2 = -\frac{v^2}{2} U_2^T Y_\nu m_R^{-1} Y_\nu^T U_2. \quad (\text{III.10})$$

Introducing the matrix

$$R = i \frac{v}{\sqrt{2}} m_R^{-1/2} Y_\nu^T U_2 (m_\nu^{\text{diag}})^{-1/2}, \quad (\text{III.11})$$

we obtain

$$R^T R = -\frac{v^2}{2} (m_\nu^{\text{diag}})^{-1/2} \left( U_2^T Y_\nu m_R^{-1/2} m_R^{-1/2} Y_\nu^T U_2 \right) (m_\nu^{\text{diag}})^{-1/2}, \quad (\text{III.12})$$

which equals the unit matrix because the expression in the parenthesis can be simplified using Eq. (III.10). The relation  $R^T R = I$  is fulfilled by any orthogonal matrix. We can solve Eq. (III.11) for the neutrino Yukawa matrix, and find

$$Y_\nu = \frac{\sqrt{2}}{v} U_2^* (m_\nu^{\text{diag}})^{1/2} (-i R^T) m_R^{1/2}. \quad (\text{III.13})$$

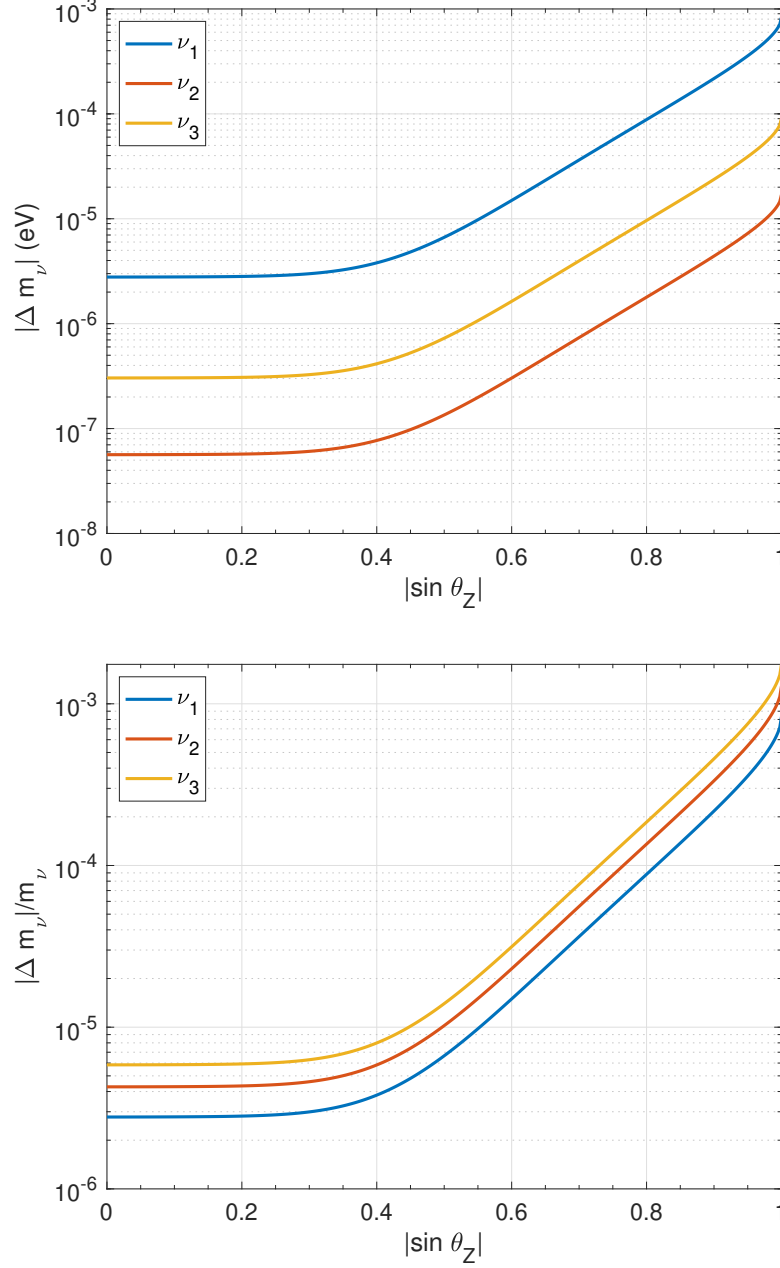


Figure 2. One-loop mass corrections to active neutrinos, for **BP1**, with  $M_{Z'} = 50 \text{ MeV}$ ,  $M_s = 250 \text{ GeV}$ ,  $\sin \theta_S = 0.1$  and  $\text{sgn}(\theta_Z) = +1$ . Top: Correction in eV units. Bottom: Correction relative to tree mass. The plot is almost identical for  $\text{sgn}(\theta_Z) = -1$ .

The inclusion of sterile neutrinos results in non-unitary active-light neutrino mixing matrix [42, 43] that we write as  $(I - \alpha)U_{\text{PMNS}}$  where the matrix  $\alpha$  is proportional to the active-sterile mixing squared, which is tiny. Hence, we neglect  $\alpha$  in this study, so the active-light mixing is described by the unitary matrix  $U_{\text{PMNS}} = U_{\ell L}^\dagger U_2$  (Pontecorvo-Maki-Nakagawa-

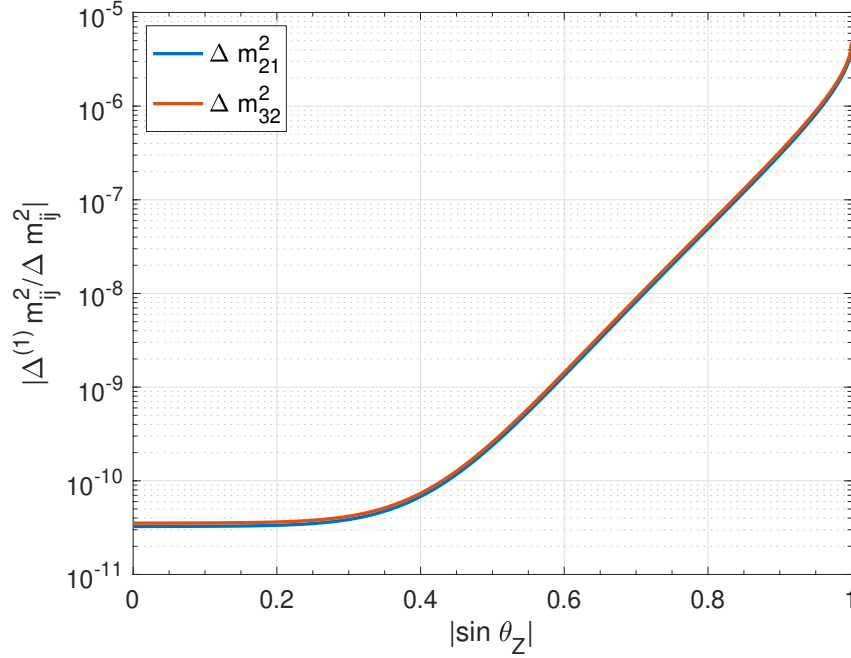


Figure 3. Relative one-loop corrections to neutrino oscillation parameters  $\Delta m_{21}^2$  and  $\Delta m_{31}^2$  with respect to tree-level parameter, for **BP1**, with  $M_{Z'} = 50$  MeV,  $M_s = 250$  GeV,  $\sin \theta_S = 0.1$  and  $\text{sgn}(\theta_Z) = +1$ .

Sakata matrix). We may choose to set  $U_{\ell L} = I$ , leading to  $U_{\text{PMNS}} = U_2$ , which is possible if we assume that the charged lepton Yukawa matrix  $Y'_\ell$  is invertible<sup>3</sup>, so the right-diagonalizing matrix is  $U_{\ell R} = (Y'_\ell)^{-1} Y_\ell$ . This choice ensures that for the charged leptons the flavour and mass eigenstates coincide. For the active neutrinos the same choice is not possible. The  $U_2$  PMNS matrix may also include the CP violating and the unknown, complex Majorana phases, but we set those to zero in this study, as we do not expect that such phases will change our conclusions significantly.

Using that  $m_R$  is real and diagonal, we can write the mixing matrix (III.5) as

$$U_{\text{as}} = \frac{v}{\sqrt{2}} Y_\nu^* m_R^{-1}. \quad (\text{III.14})$$

We substitute the matrix  $Y_\nu$  as given in Eq. (III.13) to obtain

$$U_{\text{as}} = U_{\text{PMNS}} \sqrt{m_\nu^{\text{diag}}} (iR^\dagger) m_R^{-1/2}. \quad (\text{III.15})$$

---

<sup>3</sup> Non-invertible matrices are rare in the sense that the measure of the set of given size such matrices is zero.

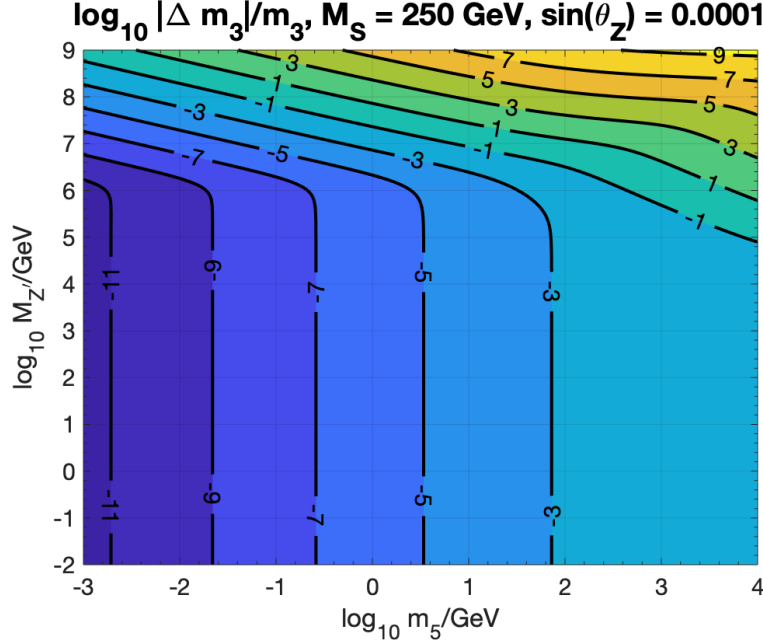


Figure 4. Relative one-loop corrections to  $m_3$  in logarithmic  $(m_5, M_{Z'})$  plane, for **BP1** with  $M_s = 250$  GeV,  $\sin \theta_S = 0.1$  and  $\sin \theta_Z = 10^{-4}$ . Contour labels  $n$  correspond to  $|\Delta m_3| = 10^n m_3$ .

We see that even though the light and heavy neutrino masses and PMNS matrix are independent of the choice of  $R$  matrix, the mixing between active and sterile neutrinos is not so. One needs to scan over the possible orthogonal matrices  $R$  to obtain suitable values of active-sterile mixing. In this exploratory study we consider real  $R$  matrices, and parameterize it with three Euler angles, whose sines we denote with  $s_{12}$ ,  $s_{13}$  and  $s_{23} \in [0, 1]$  and cosines with  $c_{ij} (= \sqrt{1 - s_{ij}^2})$ :

$$R(s_{12}, s_{13}, s_{23}) = \begin{pmatrix} c_{12}c_{13} & s_{12}c_{13} & s_{13} \\ -s_{12}c_{23} - c_{12}s_{23}s_{13} & c_{12}c_{23} - s_{12}s_{23}s_{13} & s_{23}c_{13} \\ s_{12}s_{23} - c_{12}c_{23}s_{13} & -c_{12}s_{23} - s_{12}c_{23}s_{13} & c_{23}c_{13} \end{pmatrix}. \quad (\text{III.16})$$

## IV. Nonstandard interactions

As the neutral  $Z'$  boson couples to both active neutrinos and charged fermions, it will lead to nonstandard neutrino interactions (NSI), see Fig. 5 for a relevant Feynman diagram. Integrating out the  $Z'$  boson, we find the non-renormalizable dimension-6 effective operator



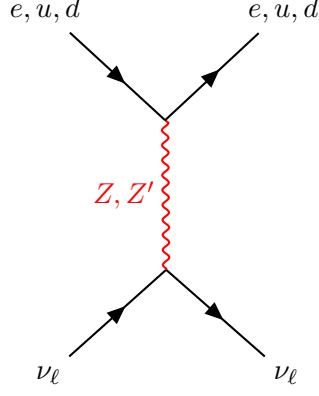


Figure 5. Neutral gauge boson exchange Feynman diagram. The  $Z'$  boson contribution is the origin of the NSI in the super-weak model.

[32]

$$\mathcal{L}_{\text{NSI}} = -2\sqrt{2}G_F \varepsilon_{\ell\ell'}^{ff',X} (\bar{\nu}_\ell \gamma^\mu P_L \nu_{\ell'}) (\bar{f}' \gamma_\mu P_X f) \quad (\text{IV.1})$$

that in general distorts the neutrino oscillation probabilities. In Eq. (IV.1)  $\ell$  and  $\ell' = e, \mu, \tau$  denote flavour indices,  $f$  and  $f'$  are any fermions,  $P_X$  ( $X = L, R$ ) are chiral projection operators and  $G_F$  is Fermi's constant. Summation over flavours, fermions and chiralities is implicitly understood. If  $f = f'$ , we denote  $\varepsilon_{\ell\ell'}^{ff',X} = \varepsilon_{\ell\ell'}^{f,X}$ . The NSI parameters  $\varepsilon_{\ell\ell'}^{ff',X}$  and  $\varepsilon_{\ell\ell'}^{f,X}$  are dimensionless, and in general can be complex numbers, but when they emerge from the super-weak force they are real. Given that  $Z'$  is light, the mass suppression will not ensure that the NSI is small. Instead, the suppression is due to the small couplings.

Man-made neutrinos are utilized in oscillation experiments. Neutrinos propagate through Earth matter, consisting of electrons, protons and neutrons (i.e. u and d quarks).  $Z'$ -mediated  $\nu\ell \rightarrow \nu\ell$  and  $\nu q \rightarrow \nu q$  scatterings will produce an extra term in the neutral current Mikheyev-Smirnov-Wolfenstein potential [44–46], which is responsible for the matter effects in neutrino oscillations. However, the  $Z'$  boson couples to neutrino flavours universally. If there were no sterile neutrinos, this would not affect oscillation probabilities, but in super-weak model this is not the case. As the full light neutrino mixing matrix  $(I - \alpha)U_{\text{PMNS}}$  is not unitary, the NSI contribution to the neutrino oscillation transition probabilities will be nonzero, but suppressed by the small absolute values of the elements of active-sterile mixing matrix  $U_{\text{as}}$ . An oscillation experiment probing matter NSI parameters will measure only effective NSI,  $\varepsilon^{\text{m,eff}} \sim \varepsilon^{\text{m}} U_{\text{as}}$ , when both NSI and nonunitary contributions are present

[47]. We see from Eq. (III.14) that for the keV, MeV and GeV scale neutrinos that we are considering, the absolute values of the elements of matrix  $U_{\text{as}}$  are much smaller than the present and near-future experimental limits on the NSI parameters. Thus we conclude that the near-future neutrino oscillation experiments will not be sensitive enough to probe NSI originating from the super-weak model (see the Appendix for more details).

The  $Z'$  boson retains the lepton universality also for charged leptons, so it will not contribute to any charged lepton flavour violating processes. The super-weak force does not affect the charged currents of the SM, so there will not be any charged current NSI operators. Also, the super-weak force does not imply the existence of flavour-changing neutral currents. Nevertheless, the existence of the  $Z'$  boson will contribute to the effective mass of the neutrinos in matter and to neutrino-electron and neutrino-quark scattering processes. In fact, in neutrino scattering experiments the NSI are not suppressed by active-sterile mixing, thus those are more sensitive to the NSI as compared to oscillation experiments, and provide the primary constraints for the super-weak model in the neutrino sector. In what follows, we explore those constraints.

### A. Nonstandard interactions in medium

The matter NSI is obtained by integrating out the  $Z'$  boson mediator in the elastic  $\nu_\ell f \rightarrow \nu_\ell f$  scattering amplitude, leading to the effective Lagrangian,

$$\mathcal{L}_{\text{NSI}} = -\frac{1}{M_{Z'}^2} (eC_{Z'\nu_\ell\nu_\ell}^{\text{L}})(eC_{Z'ff}^{\text{X}})(\bar{\nu}_\ell\gamma^\mu P_{\text{L}}\nu_\ell)(\bar{f}\gamma_\mu P_{\text{X}}f). \quad (\text{IV.2})$$

Matching Eq. (IV.2) to Eq. (IV.1) reveals the form of the effective couplings:

$$\varepsilon_{\ell\ell}^{f,\text{X}} = \frac{v^2}{2M_{Z'}^2} (eC_{Z'\nu_\ell\nu_\ell}^{\text{L}})(eC_{Z'ff}^{\text{X}}), \quad \varepsilon^f \equiv \varepsilon_{\ell\ell}^f = \varepsilon_{\ell\ell}^{f,\text{L}} + \varepsilon_{\ell\ell}^{f,\text{R}} \quad (\text{IV.3})$$

where we indicated that in the super-weak model the NSI coupling is the same for all neutrino flavours:  $\varepsilon_{ee}^f = \varepsilon_{\mu\mu}^f = \varepsilon_{\tau\tau}^f$ . In principle, flavour non-universal couplings are also possible, and would cause significantly stronger oscillation-distorting NSI and charged lepton violating decays, but we do not discuss such an option here.

As matter is electrically neutral and consists only of electrons, protons and neutrons,

summing all contributions gives

$$\begin{aligned}\varepsilon^{\text{m}} &= \varepsilon^e + 2\varepsilon^u + \varepsilon^d + \frac{N_{\text{n}}}{N_{\text{e}}}(\varepsilon^u + 2\varepsilon^d) \\ &= -\frac{v^2}{8M_{Z'}^2} \frac{N_{\text{n}}}{N_{\text{e}}} \left( g'_y \cos \theta_Z - \frac{g_{\text{L}} \sin \theta_Z}{\cos \theta_W} \right) \left( (g'_y - g'_z) \cos \theta_Z - \frac{g_{\text{L}} \sin \theta_Z}{\cos \theta_W} \right)\end{aligned}\quad (\text{IV.4})$$

where  $N_{\text{n}}$  and  $N_{\text{e}}$  are the neutron and electron number densities. Interestingly, the electron and proton contributions cancel each other, and the effective coupling is proportional to neutron density in matter.

In the small  $\theta_Z$  limit, we obtain the following approximation:

$$\varepsilon^{\text{m}} \simeq \frac{v^2}{8M_{Z'}^2} \frac{N_{\text{n}}}{N_{\text{e}}} \left[ g_{\text{L}} \sin \theta_Z \frac{2g'_y - g'_z}{\cos \theta_W} - \frac{g_{\text{L}}^2 \sin^2 \theta_Z}{\cos^2 \theta_W} - g_y'^2 + g'_y g'_z \right] \quad (\text{IV.5})$$

We can obtain a numerical estimate for the NSI strength by substituting  $v = 246.22 \text{ GeV}$ ,  $g_{\text{L}} = 0.652$  and  $\cos \theta_W = 0.8819$ :

$$\begin{aligned}\varepsilon^{\text{m}} &\simeq 0.7578 \cdot \frac{N_{\text{n}}}{N_{\text{e}}} \left( \frac{10 \text{ MeV}}{M_{Z'}} \right)^2 \\ &\times \left( \frac{\sin \theta_Z}{1.353 \cdot 10^{-4}} \frac{2g'_y - g'_z}{10^{-4}} - \left( \frac{\sin \theta_Z}{1.353 \cdot 10^{-4}} \right)^2 - \left( \frac{g'_y}{10^{-4}} \right)^2 + \frac{g'_y g'_z}{10^{-8}} \right)\end{aligned}\quad (\text{IV.6})$$

In Figs. 6 and 7 we demonstrate for a selected value of  $M_{Z'}$  that it is possible to produce small NSI. We chose  $M_{Z'} = 50 \text{ MeV}$ , within the range relevant for freeze-out dark matter production [21]. We see that the allowed region (within the  $10^{-1}$  contours) is constrained to  $-10^{-5} \lesssim \theta_Z < 10^{-4}$ . For  $\theta_Z < 0$ , small NSI is produced only if  $\tan \beta \gtrsim 1.5$ . For  $\theta_Z > 0$ , there is no constraint for  $\tan \beta$ , but for  $\tan \beta \lesssim 1.5$  there will be also a lower bound on  $\theta_Z$ , and the available range for  $\theta_Z$  shrinks to a narrow interval as  $\tan \beta$  decreases (see Fig. 6).

Increasing the mass of the  $Z'$  boson will decrease the NSI strength, and therefore the contours in Fig. 6 and Fig. 7 will move upwards. We demonstrate this behaviour in Fig. 8 for the region  $|\varepsilon^{\text{m}}| \lesssim 0.1$ . Our choice for this region is motivated by the current experimental bounds  $|\varepsilon_{\ell\ell}^{e,u,d}| \lesssim 0.1$  [48, 49]. The NSI constraint forces the gauge couplings  $g'_y$  and  $g'_z$  be quite small, less than about  $10^{-4}$ .

We conclude this subsection with a remark. Given a medium with electron density  $N_{\text{e}} = 10^{30} \text{ m}^{-3}$ , the effective neutrino mass (for all flavours in flavour-universal case) in medium is changed by

$$\Delta m_{\nu}^{\text{m}} = \sqrt{2} G_{\text{F}} N_{\text{e}} \varepsilon^{\text{m}} = V_{\text{CC}} \varepsilon^{\text{m}} \ll m_{\nu} \sim 0.01 \text{ eV}, \quad (\text{IV.7})$$

where  $V_{\text{CC}} = \text{O}(10^{-13}) \text{ eV}$  is the matter potential in the Earth and  $\text{O}(10^{-11}) \text{ eV}$  in the Sun.

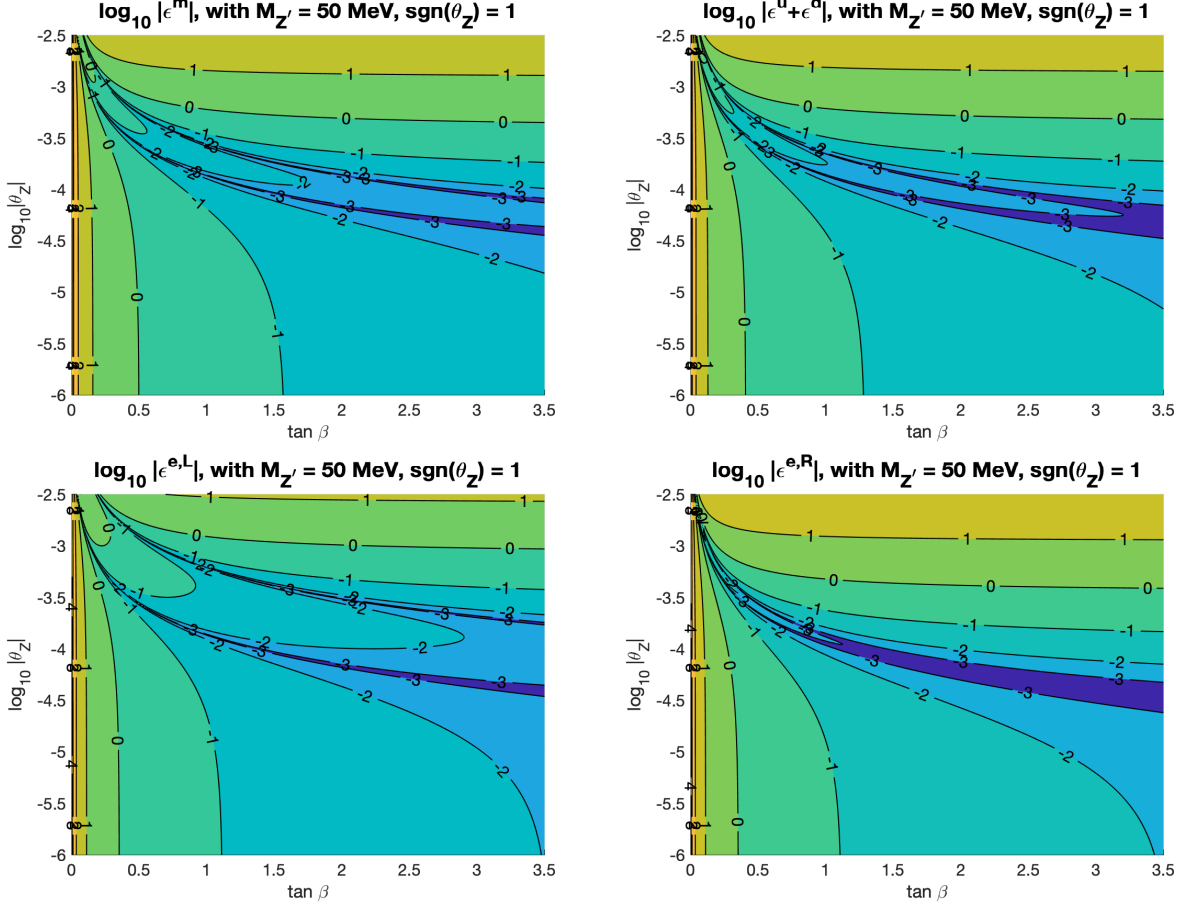


Figure 6. Contour plots of  $\log_{10} |\varepsilon^f|$  for  $\text{sgn}(\theta_Z) = +1$  in the semilogarithmic  $(\tan\beta, \log_{10} |\theta_Z|)$  plane with  $M_{Z'} = 50 \text{ MeV}$ . Contour label  $n$  corresponds to value  $\varepsilon^f = 10^n$ . Upper left: total NSI,  $\varepsilon^m$ . Upper right: quark NSI,  $\varepsilon^u + \varepsilon^d$ . Lower left: left-chiral lepton NSI,  $\varepsilon_{\ell\ell}^{e,L}$ . Lower right: right-chiral lepton NSI,  $\varepsilon_{\ell\ell}^{e,R}$ .

## B. Changes to the neutrino-electron elastic scattering

In the super-weak model, the flavour-conserving NSI gives an additional contribution to neutrino-electron elastic scattering cross section [50]:

$$\sigma(\nu_e e \rightarrow \nu_e e) = \frac{2}{\pi} G_F^2 m_e E_\nu \left( \left( 1 + g_L^e + \varepsilon_{ee}^{e,L} \right)^2 + \frac{1}{3} \left( g_R^e + \varepsilon_{ee}^{e,R} \right)^2 \right), \quad (\text{IV.8})$$

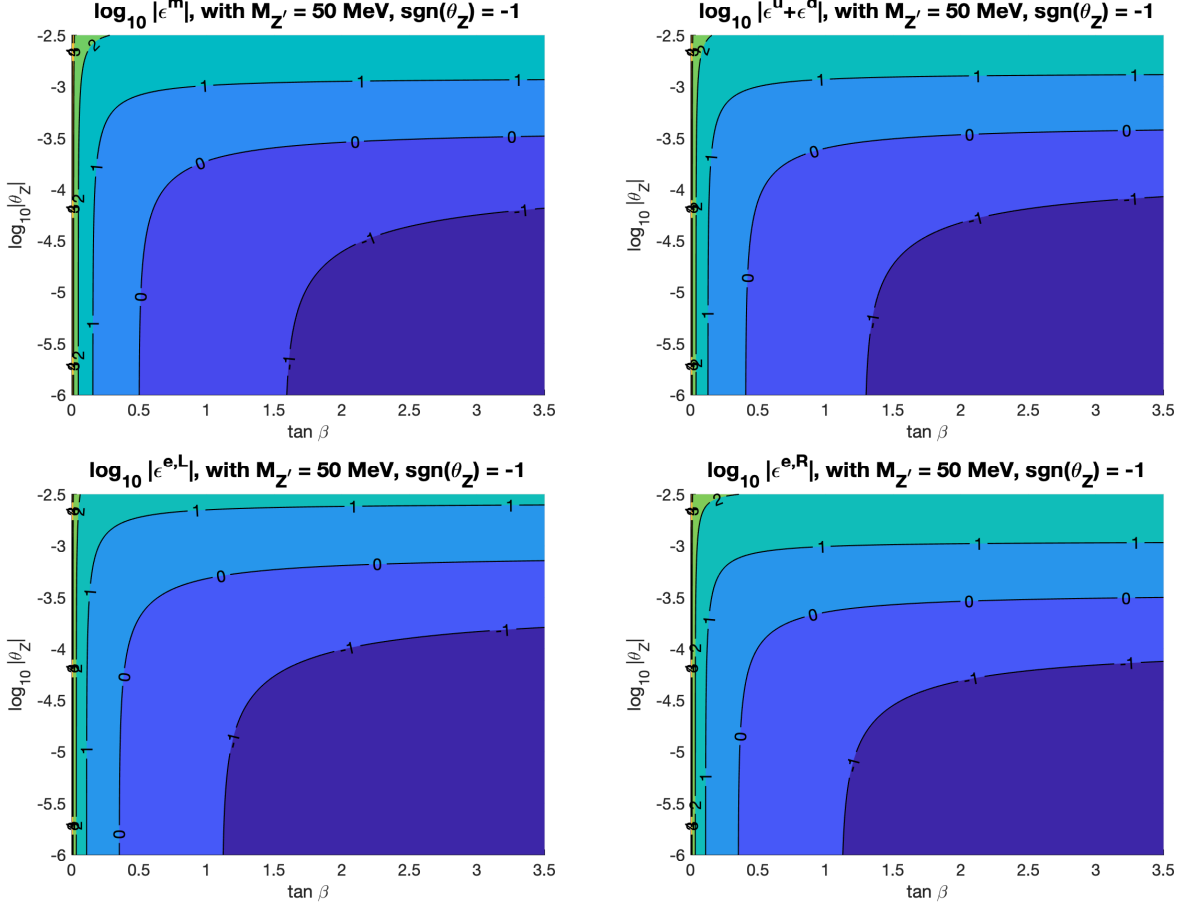


Figure 7. Same as Fig. 6, but for  $\text{sgn}(\theta_Z) = -1$ .

where the NSI couplings are

$$\begin{aligned}
\varepsilon_{ee}^{e,L} &= \frac{v^2}{8M_{Z'}^2} \left( (g'_y - g'_z) \cos \theta_Z - g_L \frac{\sin \theta_Z}{\cos \theta_W} \right) \\
&\quad \times \left( (g'_y - g'_z) \cos \theta_Z + g_L \frac{1 - 2 \sin^2 \theta_W}{\cos \theta_W} \sin \theta_Z \right) \\
\varepsilon_{ee}^{e,R} &= \frac{v^2}{8M_{Z'}^2} \left( (g'_y - g'_z) \cos \theta_Z - g_L \frac{\sin \theta_Z}{\cos \theta_W} \right) \\
&\quad \times \left( (2g'_y - 3g'_z) \cos \theta_Z - 2g_L \frac{\sin^2 \theta_W}{\cos \theta_W} \sin \theta_Z \right)
\end{aligned} \tag{IV.9}$$

Comparing these cross sections to results of scattering experiments the upper bounds  $|\varepsilon_{ee}^{e,L}|, |\varepsilon_{ee}^{e,R}| \lesssim 0.1$  are derived in Ref. [50].

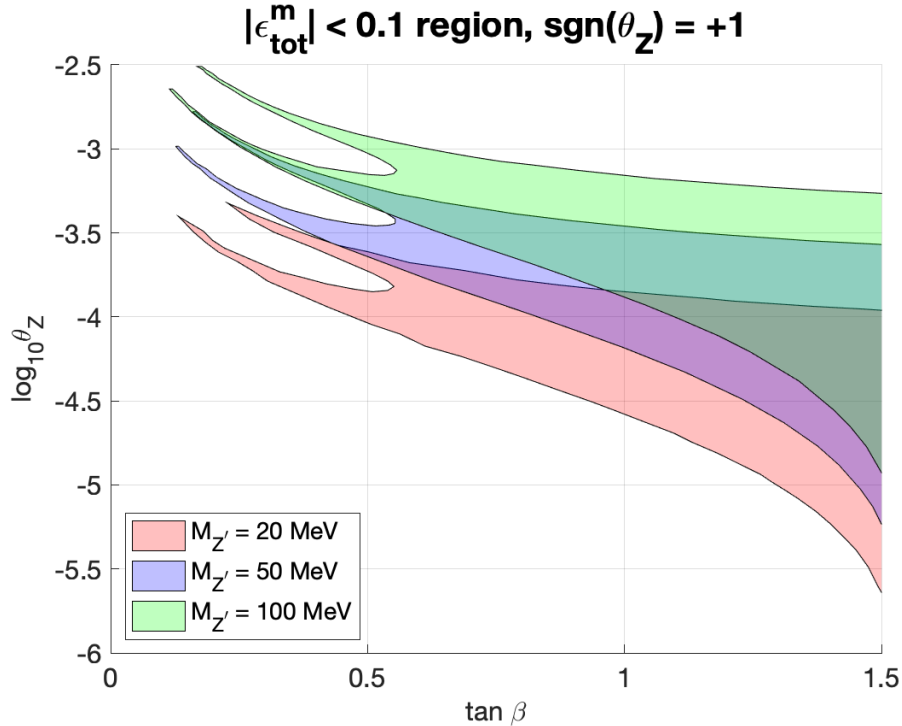


Figure 8. The available parameter space consistent with  $|\epsilon^m| < 0.1$  for  $\text{sgn}(\theta_Z) = +1$  in semi-logarithmic  $(\tan \beta, \log_{10} \theta_Z)$  plane.

## V. Benchmark points

We searched for benchmark points in the ranges  $m_1 \in [0, 50]$  meV,  $m_4 \in [1, 50]$  keV, except for **BP5** for which  $m_4$  is chosen in the MeV range where  $N_1$  can be a proper freeze-out dark matter candidate. The other benchmarks are suitable for the freeze-in case [21]. We have chosen **BP2** so that it is consistent with the unidentified 3.5 keV X-ray line. We assume almost mass-degenerate sterile neutrinos  $N_2$  and  $N_3$  with masses  $m_{5,6} \in [1, 80]$  GeV, motivated by the  $\nu$ MSM scenario [12, 13], although it is also possible to relax on this assumption of mass degeneracy. As mentioned in Sect. III, there are stringent bounds on active-sterile mixing in this mass range. For the sterile neutrino  $N_1$  with  $m_4$  in the keV range the corresponding bound is more relaxed,  $|U_{a4}|^2 \lesssim 10^{-4}$  [25]. Studies on future tritium beta decay experiments imply that the sterile- $\nu_e$  mixing bound may improve significantly to  $|U_{e4}|^2 \lesssim 10^{-8}$  [51]. Bounds for keV neutrino mixing can be set from kink searches in the  $\beta$  spectrum of radioactive nuclei, while for MeV neutrinos from peak searches from  $\pi$  and  $K$

Table III. Input values of benchmark points:  $R$  matrix parameters, neutrino masses and vacuum expectation value of the new scalar field. We assume normal mass hierarchy  $m_1 < m_2 < m_3$

Benchmark point	BP1	BP2	BP3	BP4	BP5
$s_{12}$	0.61	0.15	0.28	0.60	0.68
$s_{13}$	0.3126	0.10	0.86	0.58	0.40
$s_{23}$	0	0.40	0	0.16	1.00
$m_1$ (meV)	10	1	0	0.1	5
$m_4$ (keV)	30	7.1	40	50	25000
$m_{5,6}$ (GeV)	2.5	3.0	3.5	2.0	1.5
$w$ (GeV)	100	750	250	500	175

meson decays [26–29], and for GeV neutrinos from collider experiments, with a CMS result [52] obtained at the 13 TeV being the most constricting for  $m_{5,6} > 10$  GeV. The Future Circular Collider in the lepton collision mode will have the possibility to test a large portion of the parameter space favorable by our benchmark points.

We used  $v = 246.22$  GeV for the VEV of the scalar field  $\phi$  and  $w \in [100, 750]$  GeV for the VEV of the second scalar. In our analysis the mass of  $Z'$  boson plays a role only when we calculate the one-loop corrections to the light neutrino masses and the tree-level contributions to nonstandard interactions. The values for the Yukawa and the mixing matrices are independent of the gauge sector. The input values for each benchmark point are given in Table III. The one-loop corrections to active neutrino masses are dependent also on the gauge parameters  $g'_y$ ,  $g'_z$  and  $\theta_Z$ . These parameters do not affect any other observables in the neutrino sector. A related analysis has been carried out in Ref. [53] where the new U(1) coupling is of order unity, the mass of  $Z'$  is at the GeV scale and tree-level neutrino masses vanish.

The various accelerator, beam dump and decay search experiments constrain the combinations

$$U_e^2 = \sum_{i=4}^6 |U_{ei}|^2 \quad \text{and} \quad U_\mu^2 = \sum_{i=4}^6 |U_{\mu i}|^2 \quad (\text{V.1})$$

of the elements of the active-sterile mixing matrix  $U_{\text{as}}$ . We can use these sums to investigate the dependence of the neutrino sector of super-weak model on the  $R$  matrix, the lightest

neutrino mass  $m_1$  and the sterile neutrino masses  $m_4$ ,  $m_5$  and  $m_6$ . The sum  $U_X^2$  in Eq. (V.1) represents the weight of sterile components in  $\nu_X$  ( $X = e$  or  $\mu$ ).

We scanned the parameters of the  $R$  matrix over the whole parameter space  $(s_{12}, s_{13}, s_{23}) \in [0, 1]^3$  to enhance the active-sterile mixings  $U_e^2$  and  $U_\mu^2$  enough, so that those will be testable at different upcoming experiments. We performed systematic iterative searches by locating the optimal region in the unit cube, followed by a search again in the optimal sub-volume with a denser sampling until we reached the desired accuracy of the  $s_{ij}$  values.

All the benchmark points give valid physics scenarios, and are sensitive to different combinations of the experiments. It turns out that the (2,2), (2,3), (3,2) and (3,3) elements dominate  $Y_\nu$ , as they correspond to the heavy right-handed neutrinos  $N_2$  and  $N_3$ . Similarly, the first column in the active-sterile mixing matrix corresponds to mixing of the active neutrinos to  $N_1$ . Since  $N_1$  is at keV scale, active- $N_1$  mixing is stronger than active- $N_2$  and  $-N_3$  mixing,

$$|U_{a4}| \gg |U_{a5}|, |U_{a6}|, \quad a = e, \mu, \tau. \quad (\text{V.2})$$

The values of  $U_e^2$  and  $U_\mu^2$  at our benchmark points are presented in Table IV where we have also demonstrated that the relative one-loop corrections to the neutrino masses are at most at the per mill level. In addition, we calculated the leading order correction to the mass  $\Delta m_4$  of the lightest sterile neutrino using Eq. (III.6). The correction was found to be less than 1 %, with **BP2** being the exception where the correction is 18.5 %. The lightest sterile neutrino dominates the effective mixing as it is assumed to be lighter than the other sterile neutrinos by more than four orders of magnitude. Thus, there is no significant dependence of  $U_e^2$  and  $U_\mu^2$  on  $m_{5,6}$ . In Fig. 9 we present the expected effective mixings  $U_e^2$  and  $U_\mu^2$  as a function of the smallest sterile neutrino mass  $m_4$  at selected values of the smallest active neutrino mass  $m_1$  for points **BP1**, **BP2** and **BP5**. We know from Eq. (III.15) that the effective mixing scales as  $m_\nu^{\text{diag}} m_R^{-1}$ . Departure from the simplest choice  $R = I_3$  (i.e.  $s_{12} = s_{13} = s_{23} = 0$ ) can enhance the effective mixing to a degree where it becomes large enough to be accessible in the future experiments.

We present the current experimental bounds and sensitivities of various future experiments for sterile neutrinos over the  $(m_{5,6}, U_e^2)$  and  $(m_{5,6}, U_\mu^2)$  planes in Figs. 10 and 11. The BBN bound in the lower left corner corresponds to the maximal mean lifetime of the sterile neutrino less than 1 s, otherwise it would disrupt the big bang nucleosynthesis (BBN) in the early universe [54]. The DUNE curve (orange dashed) gives the expected 5-year sensitivity



Table IV. Output values of benchmark points: effective active-sterile mixing and neutrino mass correction. For the one-loop correction we used  $|\theta_Z| < 10^{-4}$ ,  $M_{Z'} = 20 \text{ MeV}$ ,  $M_s = 250 \text{ GeV}$  and  $\sin \theta_S = 0.1$ . Note that for **BP3** we have chosen  $m_1^{\text{tree}} = 0$ , hence  $\Delta m_1^{1\text{-loop}}/m_1^{\text{tree}}$  is undefined.

Benchmark point	BP1	BP2	BP3	BP4	BP5
$U_e^2$	$4.0 \times 10^{-7}$	$1.9 \times 10^{-7}$	$3.3 \times 10^{-8}$	$5.0 \times 10^{-8}$	$3.0 \times 10^{-10}$
$U_\mu^2$	$8.5 \times 10^{-8}$	$1.2 \times 10^{-8}$	$5.6 \times 10^{-7}$	$2.7 \times 10^{-7}$	$2.4 \times 10^{-10}$
$\Delta m_1^{1\text{-loop}} \text{ (eV)}$	$1.2 \times 10^{-5}$	$9.1 \times 10^{-8}$	0	$1.5 \times 10^{-7}$	$8.0 \times 10^{-6}$
$\Delta m_2^{1\text{-loop}} \text{ (eV)}$	$2.4 \times 10^{-5}$	$2.4 \times 10^{-5}$	$2.4 \times 10^{-5}$	$1.7 \times 10^{-5}$	$1.7 \times 10^{-5}$
$\Delta m_3^{1\text{-loop}} \text{ (eV)}$	$1.3 \times 10^{-4}$	$1.4 \times 10^{-4}$	$3.9 \times 10^{-5}$	$8.8 \times 10^{-5}$	$1.1 \times 10^{-4}$
$\Delta m_1^{1\text{-loop}}/m_1^{\text{tree}}$	$1.2 \times 10^{-3}$	$9.1 \times 10^{-5}$	undefined	$1.5 \times 10^{-3}$	$1.6 \times 10^{-3}$
$\Delta m_2^{1\text{-loop}}/m_2^{\text{tree}}$	$1.8 \times 10^{-3}$	$2.8 \times 10^{-3}$	$2.8 \times 10^{-3}$	$2.0 \times 10^{-3}$	$1.7 \times 10^{-3}$
$\Delta m_3^{1\text{-loop}}/m_3^{\text{tree}}$	$2.5 \times 10^{-3}$	$2.8 \times 10^{-3}$	$7.6 \times 10^{-4}$	$1.7 \times 10^{-3}$	$2.2 \times 10^{-3}$
$ \Delta m_4  \text{ (eV)}$	0.01	1311	212	53.0	0.008

of the DUNE near detector with  $5 \times 10^{21}$  protons on target [55]. The SHiP line (lemon dashed) represents the 90 % C.L. discovery potential of the SHiP experiment [56]. The FCC-ee exclusion curve (purple solid) assumes  $10^{12}$  Z boson decays [57]. The NA62 bound (green solid) is from Ref. [58] and the MATHUSLA bound (blue solid) from Ref. [59]. We chose the benchmark points in such a way that they all evade the present experimental bounds, but can be tested at future experiments (see the legend in Figs. 10 and 11). We have also checked that active- $N_1$  mixing satisfied the  $\beta$  decay electron energy spectrum kink bounds given in [25].

## VI. Conclusions

In this paper we studied the experimental feasibility of the neutrino sector of the super-weak U(1) extension of the standard model. We demonstrated that there exist benchmark points that are consistent with current observational constraints from neutrino oscillation and scattering experiments. At these points the lightest sterile neutrino, with mass of O(10) MeV is a viable freeze-out dark matter candidate, while with mass of O(10) keV, is

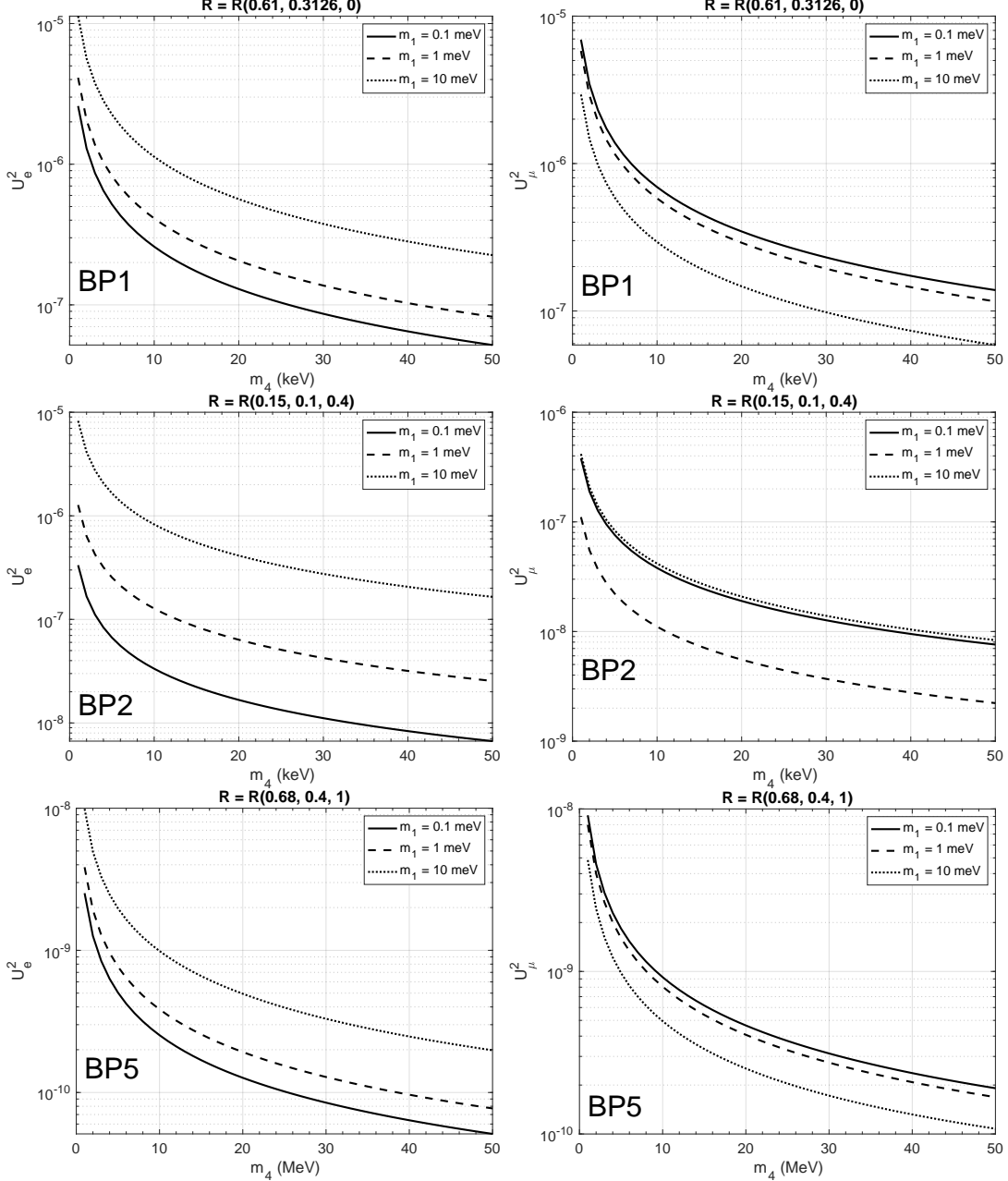


Figure 9. Left plots: effective mixing squared of electron neutrino  $\nu_e$  to sterile flavours as a function of  $m_4$  at benchmark points **BP1**, **BP2** and **BP5**. Right plots: same for  $\nu_\mu$ . We have used  $m_1 = 0.1, 1$  and  $10$  meV and normal mass hierarchy.

so in the freeze-in scenario and can also provide a possible explanation of the  $3.5$  keV X-ray line observed in galaxy spectra. The nearly degenerate heavy sterile neutrinos with mass of  $O(1)$  GeV may be probed independently by the MATHUSLA [59] and SHiP [35, 56] experiments in the future. We have shown that the one-loop corrections and seesaw

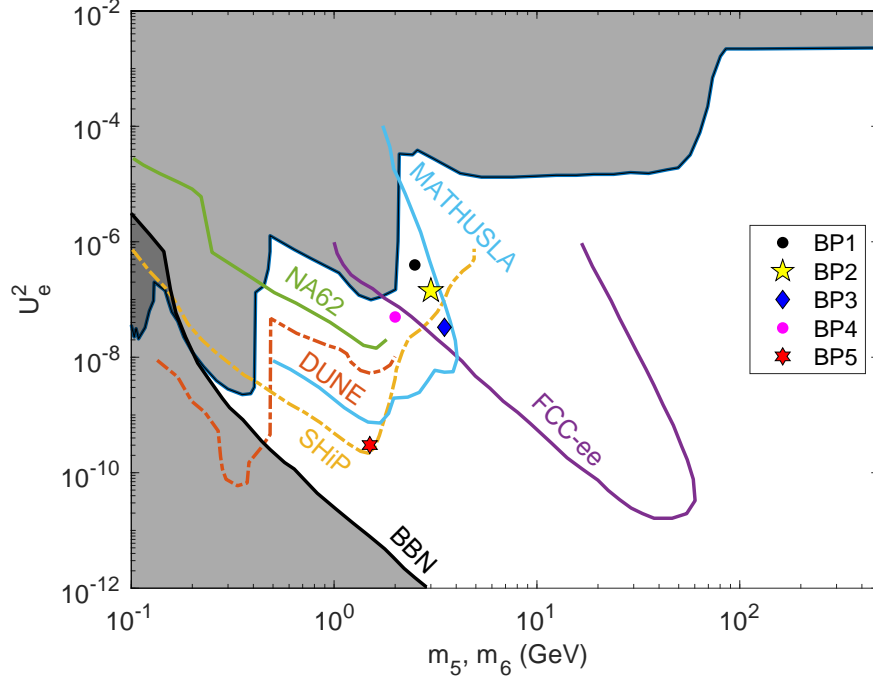


Figure 10. Constraints in logarithmic  $(U_e^2, m_i)$  plane  $i = 5, 6$  from above are given by several experiments (shaded area), collected from [35, 58, 59]. Experimental sensitivities of future experiments are given by colored lines.

expansion terms provide negligible contributions to neutrino masses with our choices of benchmark values.

The extra neutral light  $Z'$  gauge boson in the model acts as a mediator between the neutrinos and other fermions, similar to  $Z^0$  boson in the SM. This  $Z'$  boson generates flavour-universal nonstandard interactions, and their strength is consistent with current experimental limits if the gauge sector couplings  $g'_y, g'_z$  and the mixing angle  $|\theta_Z|$  are less than  $O(10^{-4})$ . Larger values are possible only within a very narrow range if  $\theta_Z > 0$ , but disfavoured if the model is to explain the origin of dark matter abundance. The NSI can be made manifest by observing deviations from the neutrino-nucleus or neutrino-electron scattering cross sections as predicted in the standard model.

We have deliberately chosen the masses of the sterile neutrinos  $N_2$  and  $N_3$  in our benchmark points such that they can fit in the  $\nu$ MSM scenario [12–14] with the exception of CP violation, which is absent in our benchmarks. In addition, we have demonstrated the compatibility of the super-weak extension with the near-future experimental sensitivity and its

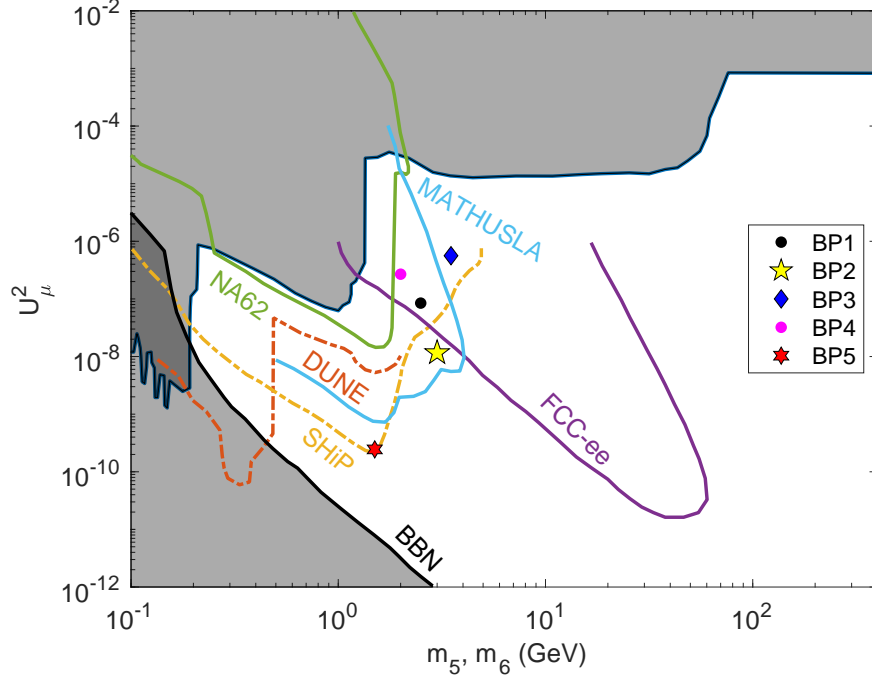


Figure 11. As in Fig. 10, but for  $U_\mu^2$ .

potential solution to the dark matter problem. Hence our conclusions motivate a detailed scan of the allowed parameter space, including non-vanishing CP phases, which we leave for later studies.

## Acknowledgments

We are grateful to Sho Iwamoto for fruitful discussions and to Josu Hernández-García for careful reading of the manuscript. This work was supported by grant K 125105 of the National Research, Development and Innovation Fund in Hungary.

## A. Flavour-universal NSI and non-unitary mixing

It is possible to perform a phase rotation in effective neutrino oscillation Hamiltonian, but it turns out that we cannot rotate away the NSI fully even if the NSI matrix

$$\varepsilon_{\text{true}} = \begin{pmatrix} \varepsilon_{ee}^m & \varepsilon_{e\mu}^m & \varepsilon_{e\tau}^m \\ \varepsilon_{\mu e}^m & \varepsilon_{\mu\mu}^m & \varepsilon_{\mu\tau}^m \\ \varepsilon_{\tau e}^m & \varepsilon_{\tau\mu}^m & \varepsilon_{\tau\tau}^m \end{pmatrix} \quad (\text{A.1})$$

is isotropic (that is, proportional to unit matrix), since the active neutrino mixing matrix, which rotates the neutrino flavour basis to neutrino mass basis, is non-unitary. Instead, the NSI is merely suppressed by unitarity deviations. The transformed NSI matrix is actually

$$\varepsilon' = N^\dagger \varepsilon_{\text{true}} N, \quad (\text{A.2})$$

where  $N$  is  $3 \times 3$  non-unitary matrix in neutrino flavour basis. In the super-weak model, the new NSI matrix is not isotropic, but the isotropic part can be isolated and removed. One gets an interesting interplay from the NSI and non-unitarity, which means in practise that in long baseline neutrino oscillations (LBNO) the effect from these two sources is indistinguishable. Consider an example: suppose we measure a 2 % distortion in neutrino oscillation probabilities, and we cannot fit it in standard three-neutrino no-BSM framework. This distortion may be caused fully by the NSI, fully by non-unitarity or by both in unknown ratio. In this case the LBNO experiments constrain only the combined effect. Short-baseline experiments in turn constrain non-unitarity.

Let  $N \equiv (I - \alpha)U_{\text{PMNS}}$  be the non-unitary neutrino mixing matrix. The deviation matrix

$$\alpha = \begin{pmatrix} \alpha_{ee} & 0 & 0 \\ \alpha_{\mu e} & \alpha_{\mu\mu} & 0 \\ \alpha_{\tau e} & \alpha_{\tau\mu} & \alpha_{\tau\tau} \end{pmatrix} \quad (\text{A.3})$$

has small elements, so we may ignore  $\mathcal{O}(\alpha^2)$  part. Thus,

$$H_{\text{NSI}} = N^\dagger \begin{pmatrix} \varepsilon & 0 & 0 \\ 0 & \varepsilon & 0 \\ 0 & 0 & \varepsilon \end{pmatrix} N \approx \varepsilon I - U_{\text{PMNS}}^\dagger (\alpha + \alpha^\dagger) U_{\text{PMNS}} \varepsilon. \quad (\text{A.4})$$

The first term is an irrelevant isotropic phase term in neutrino oscillations. The second term is neither isotropic nor diagonal. It is the leading order part of the NSI, which cannot be cancelled by phase-rotation, suppressing the NSI by about  $|\alpha| \sim |U_{\text{as}}| \lesssim 10^{-3}$ . Thus one must consider two different sets of bounds for oscillation and scattering experiments: the suppressed bounds for neutrino oscillations and unsuppressed ones for scattering.

## B. Light NSI mediator

Upon deriving the NSI operator, we integrate out the mediator by assuming that the propagator may be approximated by negative inverse mass squared:

$$\frac{1}{p^2 - M_{Z'}^2} \approx \frac{-1}{M_{Z'}^2}.$$

This is valid only if the momentum transfer in the scattering is small compared to the mass of the mediator,  $M_{Z'}$ . In neutrino propagation in matter only forward scattering interactions are relevant. In those cases the momentum transfer via mediator is zero. With nonzero momentum transfer the outgoing neutrino will be deflected away from the source-to-detector trajectory even if the momentum transfer is tiny. It is therefore possible to consider NSI with light mediators. However for scattering experiments one needs to have mediator mass at least about 10 MeV in order to have a meaningful approximation [60, 61].

- 
- [1] G. Aad *et al.* (ATLAS), Phys. Lett. **B716**, 1 (2012), arXiv:1207.7214 [hep-ex].
  - [2] S. Chatrchyan *et al.* (CMS), Phys. Lett. **B716**, 30 (2012), arXiv:1207.7235 [hep-ex].
  - [3] A. A. Aguilar-Arevalo *et al.* (MiniBooNE), Phys. Rev. Lett. **121**, 221801 (2018), arXiv:1805.12028 [hep-ex].
  - [4] B. Abi *et al.* (Muon g-2), Phys. Rev. Lett. **126**, 141801 (2021), arXiv:2104.03281 [hep-ex].
  - [5] Y. Fukuda *et al.* (Super-Kamiokande), Phys. Rev. Lett. **81**, 1562 (1998), arXiv:hep-ex/9807003 [hep-ex].
  - [6] Q. R. Ahmad *et al.* (SNO Collaboration), Phys. Rev. Lett. **87**, 071301 (2001).
  - [7] T. Yanagida, *Proceedings: Workshop on the Unified Theories and the Baryon Number in the Universe: Tsukuba, Japan, February 13-14, 1979*, Conf. Proc. **C7902131**, 95 (1979).

- [8] M. Gell-Mann, P. Ramond, and R. Slansky, *Supergravity Workshop Stony Brook, New York, September 27-28, 1979*, Conf. Proc. **C790927**, 315 (1979), arXiv:1306.4669 [hep-th].
- [9] R. N. Mohapatra and G. Senjanović, Phys. Rev. Lett. **44**, 912 (1980).
- [10] J. Schechter and J. W. F. Valle, Phys. Rev. **D22**, 2227 (1980).
- [11] S. L. Glashow, *Cargese Summer Institute: Quarks and Leptons Cargese, France, July 9-29, 1979*, NATO Sci. Ser. B **61**, 687 (1980).
- [12] T. Asaka and M. Shaposhnikov, Phys. Lett. **B620**, 17 (2005), arXiv:hep-ph/0505013 [hep-ph].
- [13] M. Shaposhnikov and I. Tkachev, Phys. Lett. **B639**, 414 (2006), arXiv:hep-ph/0604236 [hep-ph].
- [14] L. Canetti, M. Drewes, T. Frossard, and M. Shaposhnikov, Phys. Rev. **D87**, 093006 (2013), arXiv:1208.4607 [hep-ph].
- [15] A. Boyarsky, M. Drewes, T. Lasserre, S. Mertens, and O. Ruchayskiy, Prog. Part. Nucl. Phys. **104**, 1 (2019), arXiv:1807.07938 [hep-ph].
- [16] M. Drewes *et al.*, JCAP **1701**, 025 (2017), arXiv:1602.04816 [hep-ph].
- [17] K. Abazajian, G. M. Fuller, and M. Patel, Phys. Rev. **D64**, 023501 (2001), arXiv:astro-ph/0101524 [astro-ph].
- [18] K. N. Abazajian *et al.*, (2012), arXiv:1204.5379 [hep-ph].
- [19] A. D. Dolgov and S. H. Hansen, Astropart. Phys. **16**, 339 (2002), arXiv:hep-ph/0009083 [hep-ph].
- [20] E. K. Akhmedov, V. A. Rubakov, and A. Yu. Smirnov, Phys. Rev. Lett. **81**, 1359 (1998), arXiv:hep-ph/9803255 [hep-ph].
- [21] S. Iwamoto, K. Seller, and Z. Trócsányi, (2021), arXiv:2104.11248 [hep-ph].
- [22] M. Fukugita and T. Yanagida, Phys. Lett. B **174**, 45 (1986).
- [23] E. Bulbul, M. Markevitch, A. Foster, R. K. Smith, M. Loewenstein, and S. W. Randall, Astrophys. J. **789**, 13 (2014), arXiv:1402.2301 [astro-ph.CO].
- [24] A. Boyarsky, O. Ruchayskiy, D. Iakubovskiy, and J. Franse, Phys. Rev. Lett. **113**, 251301 (2014), arXiv:1402.4119 [astro-ph.CO].
- [25] A. Atre, T. Han, S. Pascoli, and B. Zhang, JHEP **05**, 030 (2009), arXiv:0901.3589 [hep-ph].
- [26] D. I. Britton *et al.*, Phys. Rev. Lett. **68**, 3000 (1992).
- [27] D. I. Britton *et al.*, Phys. Rev. D **46**, R885 (1992).
- [28] T. Yamazaki *et al.*, Conf. Proc. C **840719**, 262 (1984).

- [29] A. V. Artamonov *et al.* (E949), Phys. Rev. D **91**, 052001 (2015), [Erratum: Phys.Rev.D 91, 059903 (2015)], arXiv:1411.3963 [hep-ex].
- [30] F. Bergsma *et al.* (CHARM), Phys. Lett. **166B**, 473 (1986).
- [31] P. Abreu *et al.* (DELPHI), Z. Phys. **C74**, 57 (1997), [Erratum: Z. Phys.C75,580(1997)].
- [32] Y. Grossman, Phys. Lett. **B359**, 141 (1995), arXiv:hep-ph/9507344 [hep-ph].
- [33] Z. Trócsányi, Symmetry **12**, 107 (2020), arXiv:1812.11189 [hep-ph].
- [34] Z. Péli, I. Nándori, and Z. Trócsányi, Phys. Rev. D **101**, 063533 (2020), arXiv:1911.07082 [hep-ph].
- [35] S. Alekhin *et al.*, Rept. Prog. Phys. **79**, 124201 (2016), arXiv:1504.04855 [hep-ph].
- [36] K. Bondarenko, A. Boyarsky, D. Gorbunov, and O. Ruchayskiy, JHEP **11**, 032 (2018), arXiv:1805.08567 [hep-ph].
- [37] W. Grimus and L. Lavoura, JHEP **11**, 042 (2000), arXiv:hep-ph/0008179 [hep-ph].
- [38] N. Aghanim *et al.* (Planck), Astron. Astrophys. **641**, A6 (2020), arXiv:1807.06209 [astro-ph.CO].
- [39] M. Aker *et al.* (KATRIN), Phys. Rev. Lett. **123**, 221802 (2019), arXiv:1909.06048 [hep-ex].
- [40] S. Iwamoto, T. J. Kärkkäinen, Z. Péli, and Z. Trócsányi, (2021), arXiv:2104.14571 [hep-ph].
- [41] J. A. Casas and A. Ibarra, Nucl. Phys. **B618**, 171 (2001), arXiv:hep-ph/0103065 [hep-ph].
- [42] E. Fernandez-Martinez, M. B. Gavela, J. Lopez-Pavon, and O. Yasuda, Phys. Lett. B **649**, 427 (2007), arXiv:hep-ph/0703098.
- [43] M. Blennow and E. Fernandez-Martinez, Phys. Lett. B **704**, 223 (2011), arXiv:1107.3992 [hep-ph].
- [44] L. Wolfenstein, Phys. Rev. **D17**, 2369 (1978).
- [45] S. P. Mikheyev and A. Y. Smirnov, Yadernaya Fizika **42**, 1441 (1985).
- [46] S. P. Mikheev and A. Yu. Smirnov, Nuovo Cim. **C9**, 17 (1986).
- [47] M. Blennow, P. Coloma, E. Fernandez-Martinez, J. Hernandez-Garcia, and J. Lopez-Pavon, JHEP **04**, 153 (2017), arXiv:1609.08637 [hep-ph].
- [48] C. Biggio, M. Blennow, and E. Fernandez-Martinez, JHEP **08**, 090 (2009), arXiv:0907.0097 [hep-ph].
- [49] T. Ohlsson, Rept. Prog. Phys. **76**, 044201 (2013), arXiv:1209.2710 [hep-ph].
- [50] S. Davidson, C. Pena-Garay, N. Rius, and A. Santamaria, JHEP **03**, 011 (2003), arXiv:hep-ph/0302093.



- [51] S. Mertens, T. Lasserre, S. Groh, G. Drexlin, F. Glueck, A. Huber, A. W. P. Poon, M. Steidl, N. Steinbrink, and C. Weinheimer, JCAP **1502**, 020 (2015), arXiv:1409.0920 [physics.ins-det].
- [52] A. M. Sirunyan *et al.* (CMS), Phys. Rev. Lett. **120**, 221801 (2018), arXiv:1802.02965 [hep-ex].
- [53] P. Ballett, M. Hostert, and S. Pascoli, Phys. Rev. D **99**, 091701 (2019), arXiv:1903.07590 [hep-ph].
- [54] A. D. Dolgov, S. H. Hansen, G. Raffelt, and D. V. Semikoz, Nucl. Phys. **B590**, 562 (2000), arXiv:hep-ph/0008138 [hep-ph].
- [55] C. Adams *et al.* (LBNE), in *Snowmass 2013: Workshop on Energy Frontier Seattle, USA, June 30-July 3, 2013* (2013) arXiv:1307.7335 [hep-ex].
- [56] M. Anelli *et al.* (SHiP), (2015), arXiv:1504.04956 [physics.ins-det].
- [57] A. Blondel, E. Graverini, N. Serra, and M. Shaposhnikov (FCC-ee study Team), *Proceedings, 37th International Conference on High Energy Physics (ICHEP 2014): Valencia, Spain, July 2-9, 2014*, Nucl. Part. Phys. Proc. **273-275**, 1883 (2016), arXiv:1411.5230 [hep-ex].
- [58] M. Drewes, J. Hajer, J. Klaric, and G. Lanfranchi, JHEP **07**, 105 (2018), arXiv:1801.04207 [hep-ph].
- [59] D. Curtin *et al.*, Rept. Prog. Phys. **82**, 116201 (2019), arXiv:1806.07396 [hep-ph].
- [60] I. Esteban, M. C. Gonzalez-Garcia, M. Maltoni, I. Martinez-Soler, and J. Salvado, JHEP **08**, 180 (2018), arXiv:1805.04530 [hep-ph].
- [61] Y. Farzan and I. M. Shoemaker, JHEP **07**, 033 (2016), arXiv:1512.09147 [hep-ph].